# Polymer Chemistry

Accepted Manuscript


This is an *Accepted Manuscript*, which has been through the Royal Society of Chemistry peer review process and has been accepted for publication.

*Accepted Manuscripts* are published online shortly after acceptance, before technical editing, formatting and proof reading. Using this free service, authors can make their results available to the community, in citable form, before we publish the edited article. We will replace this *Accepted Manuscript* with the edited and formatted *Advance Article* as soon as it is available.

You can find more information about *Accepted Manuscripts* in the Information for Authors.

Please note that technical editing may introduce minor changes to the text and/or graphics, which may alter content. The journal's standard Terms & Conditions and the Ethical guidelines still apply. In no event shall the Royal Society of Chemistry be held responsible for any errors or omissions in this *Accepted Manuscript* or any consequences arising from the use of any information it contains.

ROYAL SOCIETY OF CHEMISTRY

www.rsc.org/polymers

Polymer Chemistry

Paper

# Engineered non-toxic cationic nanocarriers with photo-triggered slow-release properties†

Received 00th January 20xx,
Accepted 00th January 20xx

DOI: 10.1039/x0xx00000x

www.rsc.org/

Ionel A. Dinu,* Jason T. Duskey, Anja Car, Cornelia G. Palivan, Wolfgang Meier*

Charge density of polymers involved in drug delivery is a key parameter during cellular uptake; moreover, the nature of charged groups determines the encapsulation efficiency and nanocarrier stability. Unfortunately, the high toxicity and the burst release of loaded cargo are their major drawbacks. We have here developed a versatile strategy to design photo-responsive nanocarriers showing high stability, slow-release properties and low cytotoxicity. These delivery vehicles are intended to prolong the drug effect reducing the dose frequency, decreasing the side effects and maintaining a proper level of the drug. Diblock copolymers based on poly(dimethylsiloxane) and poly(2-dimethylaminoethyl methacrylate) containing pendant photo-cleavable 2-nitrobenzyl moieties were synthesized by atom transfer radical polymerization and post-polymerization modification, then self-assembled into nanoparticles. Dynamic light scattering and transmission electron microscopy showed that the size and morphology of nanoparticles were not affected by UV exposure. Nanoparticle cytotoxicity was evaluated in correlation to the number and nature of positively charged units. The nanocarriers containing copolymers with a longer charged block were successfully uptaken by cells and were non-toxic both before and after irradiation up to 300 μg $mL^{-1}$. The slow photo-induced release of a negatively charged molecule, sulforhodamine B, reveals that the delivery is controlled not only by the photo-triggered transformation of hydrophilic blocks from cationic to zwitterionic, but also by a combination of forces that induce the self-assembly but do not allow the disruption of nanoparticles. Results suggest that this polymeric system play a promising role as a nanocarrier for sustained, triggered drug delivery, preserving the non-toxicity after release.

## Introduction

Supramolecular structures formed by self-assembly of amphiphilic block copolymers in aqueous solution have attracted a strong scientific interest due to their ability to entrap hydrophilic and/or hydrophobic molecules. A wide variety of nanostructures with different architectures and properties have been reported, including micelles, rods, tubes, vesicles, nanogels, *etc*,[1-4] and by tuning the chemical composition of copolymers, the self-assembled structures could be designed to protect and deliver: small drugs, therapeutic macromolecules like peptides, plasmid DNA, small-interfering RNA[5-7] or to be used as nanocontainers for imaging agents.[8-10] However, to be considered as a therapeutic platform, a drug delivery system should have a high loading efficiency, an increased stability in physiological conditions, have a low toxicity and induce a low immune response, as well as release the cargo 'on demand' as a response to an applied stimulus, such as pH, temperature, or light.

Among the multitude of polymers used to entrap and deliver drugs or biologically active species, positively charge polymers play an important role because they form nanocarriers with enhanced cellular uptake, improved encapsulation efficiency and high stability. Cationic polymers, such as polyethyleneimine (PEI), have proven to be promising for the encapsulation and delivery of various anionic therapeutic compounds. Their charged nature allows for complex formations with anionic cargos, such as diclofenac, indomethacin, methrotexate, peptides, RNA and DNA, to protect, deliver, and beneficially influence cellular uptake.[11-18] Poly(2-dimethylaminoethyl methacrylate) (PDMAEMA), a cationic polymer containing pendant tertiary amino groups, was used as an alternative, because it has shown a lower toxicity (half maximal inhibitory concentration, $IC_{50}$ ~ 40 μg $mL^{-1}$) (18.3 kDa, pKa = 7.5) compared to PEI 25 kDa ($IC_{50}$ ~ 9 μg $mL^{-1}$), at physiological pH.[19] Nevertheless, an increase of gene transfection was reported by increasing PDMAEMA molecular weight, but at the expense of toxicity.[20] The increase of toxicity correlated with the increase of charge density is a common disadvantage of cationic delivery agents.[21-23] Various strategies have been adopted to optimize the efficiency of cationic polymers while still limiting toxicity.[24-27] One example is decreasing the interaction with serum and cell components by masking the surface charge of the particles serving to enhance colloidal stability and biocompatibility through PEGylation.[28,29] However, because of its polyether structure, PEG can undergo peroxidation, effectively reacting with, and damaging,

*Department of Chemistry, University of Basel, Klingelbergstrasse 80, 4056 Basel, Switzerland. E-mails: wolfgang.meier@unibas.ch; adrian.dinu@unibas.ch*
† Electronic Supplementary Information (ESI) available. See DOI: 10.1039/x0xx00000x

bioactive compounds, cells, and tissues;[30-32] moreover, under certain conditions rapid blood clearance can be observed after repeated injections with PEGylated systems.[33] Alternative routes for designing biocompatible stealth nanoparticles for drug delivery use zwitterionic repeating units for building the hydrophilic block to prevent non-specific protein adsorption from complex biological media.[34-36] To improve the encapsulation efficiency and stability of cationic nanocarriers while keeping the charge density as low as possible to not induce cytotoxicity, a new approach was reported. This strategy involves the increase in hydrophobicity of the polymer by introduction of poly(dimethysiloxane) (PDMS), for example, as a hydrophobic block in combination with PDMAEMA as cationic block.[23] PDMS is non-toxic, biocompatible, physiological inert, has a high oxidative stability and an extremely high backbone flexibility.[37,38] In this context, using block copolymers containing PDMS as hydrophobic block increases the stability of self-assembled structures,[39] making them ideal candidates for medical applications, such as drug-delivery or biosensing.[4,40]

Besides the high stability and low toxicity of nanocarriers modulated by chemical composition of nanostructure-forming polymers, another key role plays the ability of the self-assembled system to release the active species in a controlled manner. Hence, the increased interest for designing and development of different stimuli-responsive polymeric systems to control the release of drugs upon applying an external stimulus.[41-45] Among them, light-triggered release of the payload, which induces the photo-cleavage of the chemically attached drug or of the self-assembled polymeric structure, is an attractive, irreversible, and highly selective option.[36,46-51] One interesting example of photo-cleavable polymers used for controlled drug delivery is represented by polymers containing quaternary ammonium groups with photo-labile pendant moieties, which undergo a transformation to the zwitterionic form upon irradiation with UV light at a wavelength of 365 nm.[36,52,53]

Cationic homopolymers containing pendant tertiary amino groups, such as PDMAEMA, are pH-dependent polyelectrolytes. By quaternization, they form cationic homopolymers with fixed, permanent charges, which allows them to bind anionic payloads without any leakage induced by changes in pH of the medium. Unfortunately, after the cargo is released, the positively charged polymers can still lead to cell toxicity. In a previous investigation on nanoparticles prepared by self-assembly of pH-responsive PDMS-*b*-PDMAEMA copolymers, an increased cytotoxicity of the self-assembled nanoparticles was observed when copolymers containing a PDMAEMA block longer than five repeating units were used.[23] To overcome the toxicity caused by the increased number of positive charges, photo-sensitive homopolymers were designed to mediate, for example, the condensation of DNA into stable polyplex nanoparticles followed by the controlled release of the cargo, where the photo-induced cleavage converts the cationic homopolymer into the zwitterionic, and non-toxic, form, leading to a fast release of the payload.[52-54] So far, most of the cationic photo-responsive nanoparticulates used for controlled drug release do not last long enough and disassemble after the stimulus is applied, and consequently, a pronounced burst release is observed.[52-56]

Here, we present a simple strategy to obtain cationic delivery systems by self-assembly of positively charged photo-responsive block copolymers which can irreversibly change to a neutral form after the stimulus is applied to slowly release its cargo and remain non-toxic. To this end, two quaternized diblock PDMS-*b*-PDMAEMA copolymers with pendant photo-cleavable 2-nitrobenzyl moieties in the hydrophilic PDMAEMA block were synthesized by atom transfer radical polymerization (ATRP) followed by post-polymerization modification, then self-assembled into nanoparticles. Formation of block copolymers containing quaternary amine groups in the hydrophilic block is desired, because they provide permanent positive charges within the polymer chains. Thus, they will not lose their cationic character during pH variation, which could induce the leakage of the drug out of the nanoparticles, as in the case of nanocarriers containing polymers with tertiary amine groups. Moreover, the presence of photo-cleavable groups allows the UV light to trigger 'on demand' structural changes within the structure of cationic diblock copolymers leading to neutral polymers with no toxic effects on cells after drug release (Scheme 1).

The key function we introduce by our delivery platform consists of a slow, sustained drug release and a photo-responsive property that is intensively required for treatment of many chronic conditions in order to prolong the effect of drug at the target site and to offer a better compliance and safety for the patient.[57] In this respect, the hydrophobic counterpart of our amphiphilic block copolymers is intended to induce not only an enhanced stability to the self-assembled delivery vehicles, but a prolonged therapeutic effect after the application of stimulus by slow-release of the drug. To understand how is the delivery process controlled by the architecture of self-assembled nanoparticles and structural transformation of the hydrophilic block from cationic to zwitterionic, upon UV irradiation, the entrapment and release of a small negatively charged dye (sulforhodamine B – SRB), used as anionic model drug, were investigated.

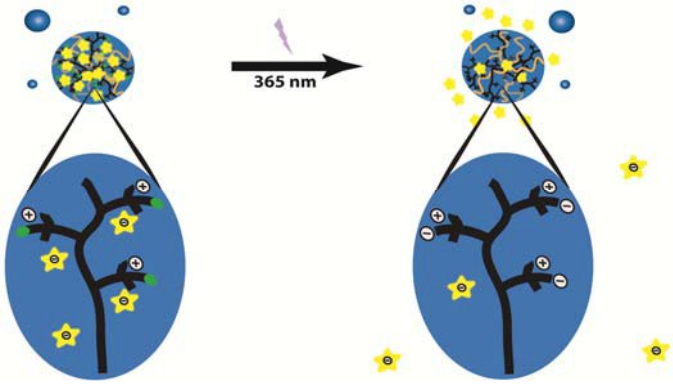


**Scheme 1.** Illustration on the photo-triggered sustained-release mechanism of anionic cargos from cationic self-assembled nanocarriers.

Our photo-responsive quaternized PDMS-*b*-PDMAEMA polymeric systems contain the benefits of complexing and delivering negatively charged payloads, while improving their specificity by stimuli-controlled (photo-mediated) sustained release, as well as minimizing toxicity at similar concentrations to other cationic polymers.

## Experimental

### Materials

Monocarbinol-terminated PDMS ($M_w$ = 5000 g $mol^{-1}$) was purchased from ABCR (Germany). 2-dimethylaminoethyl methacrylate, α-bromoisobutyryl bromide, 2-acetylpyridine (99%), propylamine (99%), 2-nitrobenzyl alcohol (97%), chloroacetic acid (99%), 1-chloropropane (98%), triethylamine (TEA), silica gel, basic alumina, sulforhodamine B (SRB), Dulbecco's phosphate buffered saline (PBS), the organic solvents, inorganic salts and acids involved in this work were purchased from Sigma-Aldrich (Germany). Dulbecco's Modified Eagle's Medium (DMEM) and HeLa cells were purchased from Sigma-Aldrich (USA). PENNstrep, trypsin, and FCS were purchased from Gibco Life Technologies. Pyridine-2-carboxaldehyde (99%) was purchased from Alfa Aesar (Switzerland). MTS (3-(4,5-dimethylthiazol-2-yl)-5-(3-carboxymethoxyphenyl)-2-(4-sulfophenyl)-2H-tetrazolium) assay was purchased from Promega (USA).

Dialysis was done in Spectra-Por Biotech-Grade CE dialysis tubes (molecular weight cut-off (MWCO) 100 kD) from Spectrum Labs (Germany), and dye release studies were performed using Spectra-Por Float-A-Lyzers (1 mL, MWCO 100 kDa) from Sigma-Aldrich (USA). Track-etched polycarbonate membranes (0.2 µm pore size) were purchased from Nuclepore (Whatman, UK). All reagents were of the highest commercially available grade and used without any further purification, unless stated otherwise. Syringe Millex-FH filters (0.45 µm pore size, hydrophobic PTFE membrane) were purchased from Merck Millipore (Germany).

Since some of the solvents and chemicals are toxic both by contact and inhalation, they should be manipulated under a chemical hood.

### Synthesis of PDMS-*b*-PDMAEMA diblock copolymers

PDMS-*b*-PDMAEMA diblock copolymers (ABn) were synthesized by atom transfer radical polymerization (ATRP) according to a previously described procedure,[23] where A represents the hydrophobic PDMS block with an average number of 65 repeating units (from $^1$H-NMR spectrum of monocarbinol-terminated PDMS), and B is the hydrophilic PDMAEMA block. The number of hydrophilic (DMAEMA) repeating units, n, was determined from the $^1$H-NMR spectra of ABn diblock copolymers. Briefly, a monofunctional PDMS-Br macroinitiator ($M_n$ = 4650 g $mol^{-1}$, PDI = 1.39, Figure S1) was synthesized from the corresponding monocarbinol-terminated PDMS using α-bromoisobutyryl bromide and TEA (molar ratio of 1:3:6) solubilized in anhydrous THF to a final polymer concentration of 10 wt.%. First, TEA was added to the PDMS solution, followed by the drop-wise addition of α-bromoisobutyryl bromide. The reaction mixture was continuously stirred at room temperature for 18 h, filtered to remove the ammonium salt, and then THF was removed under vacuum on a rotary evaporator. Afterwards, the macroinitiator was dissolved in dichloromethane and washed with a saturated $NaHCO_3$ solution. After filtration and removal of dichloromethane on rotary evaporator, the macroinitiator was repeatedly washed with methanol in a separatory funnel, changing the solution from yellow to colourless. Finally, residual methanol was removed under vacuum on a Schlenk line.

The inhibitor present in DMAEMA was removed by passing the monomer through a basic alumina column prior to use. The ATRP reaction of DMAEMA was mediated by copper (I) bromide/N-(N-propyl)-2-pyridylmethanimine complex in a toluene solution at 90 °C for 3.5-5 h, the ligand being synthesized from 2-acetylpyridine and propylamine, according to previous literature.[58] Molar ratios among the PDMS-Br macroinitiator, copper (I) bromide, and ligand were kept constant during polymerization (1:1:2), and the amount of DMAEMA monomer was varied according to the degree of polymerization. Upon completion of the reaction, the copper/ligand complex was removed by passing the reaction mixture through a basic alumina column. Finally, the copolymer products were obtained by removing the solvent with a rotary evaporator. The characteristics of the diblock copolymers were as follows: AB5, ($M_n$ = 5450 g $mol^{-1}$; PDI = 1.43), and AB27 ($M_n$ = 8900 g $mol^{-1}$; PDI = 1.46), respectively.

### Quaternization of PDMS-*b*-PDMAEMA diblock copolymers

The PDMS-b-PDMAEMA diblock copolymers with 5 and 27 DMAEMA repeating units were modified with 2-nitrobenzyl-2-chloroacetate (CANBE) and 1-chloropropane as quaternization reagents. CANBE, which was used to generate photo-labile pendant moieties, was synthesized according to the literature.[59] Briefly, 2-nitrobenzyl alcohol and chloroacetic acid were dissolved in anhydrous toluene, followed by the addition of concentrated sulphuric acid and reacted for 48 h at 85 °C. The reaction mixture was washed with water, aqueous sodium bicarbonate, again with water, then brine, and finally dried under vacuum. The solid residue was dissolved in a mixture of hexane and ethyl acetate (6:1, v:v) and purified by silica gel chromatography. The eluate was recovered and dried under vacuum, yielding light yellow oil as final product (Figure S2).

Additionally, the photo-labile diblock copolymers were prepared following a previous procedure reported for homopolymers based on poly(3-dimethylaminopropyl methacrylamide), with slight modifications.[52] Briefly, the starting ABn diblock copolymers were dissolved in an anhydrous dimethylformamide/ethyl acetate mixture (4:1 v:v). A 10 wt.% excess of CANBE was then added to the copolymer solution taking into account the molar content of DMAEMA repeating units and continuously stirred in an oil bath at 40°C. After 50 h, the reaction mixture was cooled down to room temperature, dried under high vacuum, dissolved in ethanol, and dialyzed for 24 h against ethanol (exchanged every three hours). The final product was obtained removing the ethanol

on a rotary evaporator yielding a yellow wax. The photo-labile diblock copolymers (ABQn) were protected from light exposure during all steps of synthesis, purification, and storage to avoid degradation. In addition, to investigate the influence of substituent from the pendant positively charged groups on polymer self-assembly and cytotoxicity, quaternization with 1-chloropropane was performed using a similar protocol, leading to cationic ABQPn diblock copolymers (Figures S3 and S4).

**Proton nuclear magnetic resonance ($^1$H-NMR) spectroscopy and gel permeation chromatography (GPC) of diblock copolymers**

$^1$H-NMR spectra were recorded at 25 °C using a Bruker 400 MHz spectrometer. Sixty-four scans were averaged per spectrum, and the copolymers were dissolved in $CDCl_3$ or DMSO-$d_6$. The composition and number average molecular weight ($M_n$) of pristine ABn copolymers were determined from the characteristic proton signals of each block (the integral of peak "d" from Figure S1 $^1$H-NMR spectrum was taken into account for calculation).[23] The $^1$H-NMR spectra of ABQn and ABQPn diblock copolymers were recorded in a similar manner, but a prefiltration step was added before measurements for block copolymers with a longer cationic block (ABQ27 and ABQP27), due to the low solubility of charged blocks in $CDCl_3$. Thus, block copolymer solutions were passed through syringe filters (0.45 µm pore size, hydrophobic PTFE membrane) to remove the small aggregates. Even though the PDMS block is not soluble in DMSO, inducing the self-assembly of block copolymers, the $^1$H-NMR characterization in DMSO-$d_6$ was performed to better investigate the changes in the hydrophilic blocks after quaternization (Figure S5).

GPC experiments were performed on a GPCmax/TDA 305 system (Viscotek/Malvern) equipped with three PLgel columns (3 µm guard column followed by two Mixed-C 5 µm columns from Agilent Technologies Chromatography Division, Germany). THF was used as the eluent at 40 °C and a flow rate of 1.0 mL min$^{-1}$. Molecular weight distributions were assessed using a calibration plot constructed with monodisperse polystyrene standards.

All measurements, including those for the kinetics investigated by $^1$H-NMR spectroscopy, were done in triplicates.

**Preparation of self-assembled nanoparticles and dye entrapment**

Self-assembled nanoparticles were obtained from starting PDMS-*b*-PDMAEMA (ABn) or quaternized PDMS-*b*-PDMAEMA (ABQn and ABQPn) diblock copolymers by a film rehydration method using an initial concentration of 3 mg mL$^{-1}$ of polymer in chloroform. Due to the reduced solubility of ABQ27 and ABQP27 in chloroform, the ABQn and ABQPn films were prepared from the corresponding ethanol solutions. After solvent evaporation, PBS buffer (pH = 7.4) was added to the polymer films. The samples were exposed for 1 min to an ultrasound bath to facilitate the transfer of polymer films into the liquid phase. Afterwards, the polymer dispersions were magnetically stirred overnight (18 h), at 300 rpm and room temperature, then extruded through a 0.2 µm track-etched polycarbonate membrane using a Mini-Extruder from Avanti Polar Lipids (USA). No precipitation was observed in the PBS dispersions after the sonication and stirring steps; moreover, no aggregates were detected on the track-etched membrane after extrusion.

SRB-loaded nanoparticles were prepared in a similar way as described above, but instead of neat PBS buffer, a 35 µmoL L$^{-1}$ solution of SRB in PBS was added to the polymer film for rehydration. Moreover, the suspension containing SRB-loaded nanoparticles were not extruded to keep constant the content of polymer and encapsulated dye, respectively.

**Characterization of self-assembled nanoparticles**

Transmission electron microscopy (TEM) measurements were performed on a Philips EM400 electron microscope operated at 100 kV. 5 µL of copolymer solution (0.06 mg mL$^{-1}$) were adsorbed on glow-discharged carbon-coated copper grids, and negatively stained with 2% uranyl acetate solution. Excess solution was blotted away using a strip of filter paper and the samples were allowed to dry in atmosphere at room temperature before observation.

Dynamic light scattering (DLS) and zeta potential measurements were performed using a Zetasizer nano ZSP (Malvern Instruments) equipped with a 10 mW He–Ne laser at a wavelength of 633 nm and a detection angle of 173°. The correlation functions were integrated using the CONTIN algorithm in order to obtain the intensity-averaged and number-averaged size distributions of the self-assemblies and polydispersity indices. The temperature during measurements was kept at 25.0 ± 0.1°C. The polymer concentration was 1 mg mL$^{-1}$ and each measurement was repeated at least three times with an equilibration time of 2 minutes before starting the measurement.

**UV irradiation**

To investigate the degradation of block copolymers by exposure to UV light and the effect of irradiation on morphology of nanoparticles, photolysis experiments were performed in triplicates using a Hamamatsu LC4 UV mercury/xenon lamp optically filtered to isolate a 365 nm band.[49] This wavelength was chosen because it is least harmful to cells,[60] but still induces the degradation of nitrobenzyl groups. The distance from the source was 5 cm, and the light intensity on each sample was 10 mW cm$^{-2}$, measured with an OAI Model 308 UV Intensity/Power Meter from S.P.S. Vertriebs GmbH (Germany).

For the kinetics studies, 10 mg copolymer was dissolved or dispersed in 1 mL $CDCl_3$ or DMSO-$d_6$, then irradiated with UV light ($\lambda$ = 365 nm) over time points between 0-60 min at room temperature, and measured by $^1$H-NMR spectroscopy. The recorded data were fit to a first order exponential equation $y = y_0 + Ae^{-kt}$ using least squares regression, where $k$ is the pseudo-first order constant rate of the photo-degradation reaction.[61] The percent of cleavage was calculated as the variation of corresponding integral of the signal in time, taking as reference a signal with a constant integral over the same interval of time.

Additionally, the kinetics of photo-degradation was followed by UV-Vis spectroscopy on 1 mg ml$^{-1}$ photo-sensitive copolymer solutions in EtOH or nanoparticle dispersions in PBS (Figure S6). The absorbance values were acquired on a Specord

210 Plus instrument (Analytik Jena AG, Germany), as a spectral scan between λ = 250 nm and λ = 550 nm (Δλ = 1 nm), with a scan speed of 2 nm $s^{-1}$, at room temperature. In this range of wavelengths only the photo-cleavable copolymers show an absorbance maximum characteristic to 2-nitrobenzyl moieties.

**Cell culture and viability MTS assay**

HeLa cells (5'000 cells per well) were seeded in a 96-well plate Lab-Tek™ (Nalge Nunc International, USA), and incubated at 37 °C, 5% $CO_2$ for 24 h in DMEM containing 10% fetal calf serum and 1% Penicillin/Streptomycin. At 24 hours, polymer nanoparticles suspended in PBS (preparation same as previously stated at 3 mg $mL^{-1}$) were added to triplicate wells containing 100 µL per well (90 µL media supplemented with 10 µL particle suspension made in PBS) at concentrations ranging from 50-400 µg $mL^{-1}$ and incubated for an additional 24 h. Cell growth inhibition was measured using the MTS assay: 20 µL MTS assay solution was added to each well and incubated for 3 hours at 37 °C as per the supplier's instructions. Cell viability was determined by absorbance at 490 nm of each well measured with a microplate reader (SpectraMax M5$^e$, Molecular Devices, USA) and calculated as a percent of live cells compared to a PBS control (100% cell viability). All samples were corrected against controls containing only media and PBS.

***In vitro* dye release.**

The release profile of SRB was studied by UV-Vis and fluorescence spectroscopy. In general, 2 mL of SRB-loaded nanoparticle suspension (3 mg $mL^{-1}$ copolymer film rehydrated with 35 µmoL $L^{-1}$ solution of SRB in PBS) was placed in a dialysis tube (MWCO 100 kDa) and immersed in 1 L of PBS. The solution was stirred at 300 rpm in the dark at 4°C. The dialysis buffer was exchanged every three hours over the first 12 h and every 6 h after for 36 h. To ensure the free dye was completely removed, the SRB-loaded nanoparticle suspension was dialyzed for three more days, measuring the absorbance and fluorescence every 24 h. The presence of ABn copolymer chains in the SRB aqueous solution did not influence the position and intensity of SRB characteristic absorption maximum in the UV-Vis spectra ($\lambda_{max}$ = 565 nm, in PBS). Therefore, the amount of entrapped SRB was calculated from the absorbance values taking into account the extinction coefficient of SRB (ε = (9.54 ± 0.14) × $10^4$ $M^{-1}$ $cm^{-1}$) determined from the standard calibration plot (Figure S8). A sharp decrease of the SRB absorption maximum was observed in the presence of ABQn copolymers due to the interaction of negatively charged dye with the oppositely charged groups of the block copolymers (methacromatic behavior). In this case, the amount of entrapped SRB was determined by taking into account the extinction coefficient corresponding to ABQn-SRB complex (ε = (5.27 ± 0.24) × $10^4$ $M^{-1}$ $cm^{-1}$) (Figure S8).

The dye loading efficiency (DLE) was calculated using the equation (1):

$$\mathrm{DLE}\ [\%] = \frac{m_{entrapped}}{m_{feed}} \times 100 \qquad (1)$$

where: $m_{entrapped}$ is the weight of entrapped SRB into nanocarrier; and $m_{feed}$ is the weight of SRB in the feed.

*In vitro* dye release from loaded ABQn nanoparticles was investigated in PBS buffer. The purified SRB-loaded nanoparticle suspension was split in two equal volumes. Half of the solution was exposed to UV light (λ = 365 nm) at room temperature for 30 minutes. After that, it was introduced into a Spectra-Por Float-A-Lyzer (1 mL, MWCO 100 kDa) and dialyzed against 80 mL PBS buffer. The dialysis buffer was exchanged every three hours within the first 12 h and every 6 h after that for 12 h. The other half was kept as non-cleaved control and was dialyzed in the same manner in the dark. The residual dye content that remained in the dialysis tube was evaluated by UV-Vis measurements at 565 nm, taking into account the extinction coefficient corresponding to ABQ27-SRB complex (ε = (5.27 ± 0.24) × $10^4$ $M^{-1}$ $cm^{-1}$).

The percent of released dye (DRE) was determined using the equation (2):

$$\mathrm{DRE}\ [\%] = \frac{m_{entrapped} - m_{resdual}}{m_{entrapped}} \times 100 \qquad (2)$$

where: $m_{entrapped}$ is the weight of entrapped SRB into nanocarriers; $m_{residual}$ is the weight of residual SRB into irradiated nanoparticles.

Furthermore, the release kinetics of SRB was studied by fluorescence spectroscopy. The dye release protocol was similar, and samples were measured with a LS55 Luminescence Spectrometer (Perkin Elmer) using a 1 mm QS cuvette in a 90° arrangement. Briefly, purified SRB-loaded nanoparticle dispersion was split in two equal volumes: one was irradiated for 30 minutes while the second was kept in the dark. Afterwards, both of them were dialyzed against PBS buffer. The samples were excited at λ = 540 nm and emission was monitored at λ = 580 nm (7.5 nm slits). *In vitro* dye release from loaded ABQn nanoparticles was investigated in PBS buffer after 24 h, 48 h, and 72 h respectively, and then their fluorescence was compared with those corresponding to non-irradiated samples.

All dye release experiments investigated by UV-Vis spectroscopy and fluorimetry were done in triplicates (n = 3).

**Cellular uptake of SRB-loaded ABQn nanoparticles**

HeLa cells were cultured at a density of 20'000 cells per well in an 8 well plates Lab-Tek™ (Nalge Nunc International, USA) and incubated as described previously for 24 hours. After, 24 h, 200 µg or 400 µg of SRB-loaded ABQ27 nanoparticles, without pre-irradiation or after 30 minutes of pre-irradiation, were added to each well and incubated for another 24 h. Finally, cells membrane and nuclei were stained with Hoechst (Blue channel) and Cell Deep mask Red (Green Channel) for 10 min, and visualized with a confocal laser scanning microscope (CLSM, Carl Zeiss LSM510, Germany) equipped with a 63× water emulsion lens (Olympus, Japan) for uptaken of SRB-loaded particles (Red Channel).

## Results and discussion

### Synthesis and characterization of photo-cleavable PDMS-*b*-PDMAEMA$_n$ block copolymers

To produce amphiphilic diblock copolymers with permanent positive charges, quaternary amine groups were selected to be introduced as side chains in the hydrophilic block. In addition, the presence of photo-cleavable groups will serve to trigger structural changes such to both release the entrapped molecules and lead to neutral copolymers with no toxicity.

ABn diblock copolymers with hydrophilic PDMAEMA block lengths of 5 and 27 repeating units, synthesized using a previously described procedure,[23] were used to obtain block copolymers bearing photo-labile pendant moieties (ABQn copolymers, Scheme 2) via a quaternization reaction of the tertiary amine groups with 2-nitrobenzyl 2-chloroacetate (CANBE). As a control, quaternization of the pristine ABn diblock copolymers with 1-chloropropane (ABQPn) was performed (Scheme 2).The quaternization of ABn diblock copolymers was followed by $^1$H-NMR spectroscopy.

The pristine and quaternized diblock copolymers with 27 repeating units in the hydrophilic block (AB27 and ABQ27) were selected to evaluate the modification of ABn copolymers with CANBE by analysis of $^1$H-NMR spectra (Figures 1 and S5). The corresponding $^1$H-NMR spectra for the pristine diblock copolymer with 5 repeating units in the hydrophilic block (AB5) and for propyl-quaternized diblock copolymers (ABQP5 and ABQP27) were also recorded (Figures S3 and S4).

The $^1$H-NMR spectra of AB27 and ABQ27 in $CDCl_3$ show that the signals corresponding to the protons of methyl (-N($C\underline{H}_3$)$_2$; $\delta$ = 2.2-2.5 ppm, peak 1) and methylene (-$C\underline{H}_2$-N($CH_3$)$_2$; $\delta$ = 2.5-2.8 ppm, peak 2, and -O-$C\underline{H}_2$-$CH_2$-, $\delta$ = 4.0-4.2 ppm, peak 3) groups from the pristine copolymer, AB27, (Figure 1, top spectrum) were affected by the introduction of nitrobenzyl ester group into the side chain moiety (Figure 1, bottom spectrum). Thus, the signals corresponding to these protons were not only shifted after quaternization ($\delta$ = 3.7-3.8 ppm (peaks 2, 3), and 3.4-3.5 ppm (peak 1) respectively) due to the electron-withdrawing effect of ester group (Figure 1, bottom spectrum), but were significantly decreased in intensity because of poor solubility of charged groups. Moreover, a similar behaviour was observed in the $^1$H-NMR spectra of photo-cleavable copolymers in DMSO-$d_6$, where the signals corresponding to the protons of methylene groups were decreased and shifted to 4.0-4.6 ppm, while those of methyl groups are visible at 3.5 ppm just as a shoulder of the DMSO peak (Figure S4).

However, the new signal at $\delta$ = 5.64 ppm attributed to the protons of the methylene groups which connects the pendant ester bond to the nitrogen atom (-$N^+(CH_3)_2$-$C\underline{H}_2$-CO-O-) confirms the modification of tertiary amine groups (ABQ27, Figure 1, bottom, peak 4). Concurrently, the successful quaternization of DMAEMA units can be proven by the presence of characteristic signals for the aromatic protons belonging to 2-nitrobenzyl groups in the range 7.4-8.2 ppm (Figure 1, bottom, peaks 6-9), as well as the signal at $\delta$ = 4.99 ppm (Figure 1, bottom, peak 5), corresponding to the protons of methylene group bound to the aromatic ring (-CO-O-$C\underline{H}_2$-$C_6H_4$-$NO_2$). Both peaks are also present at 5.60 and 4.82 ppm, respectively, in the $^1$H-NMR spectra measured in DMSO-$d_6$ (Figure S4).

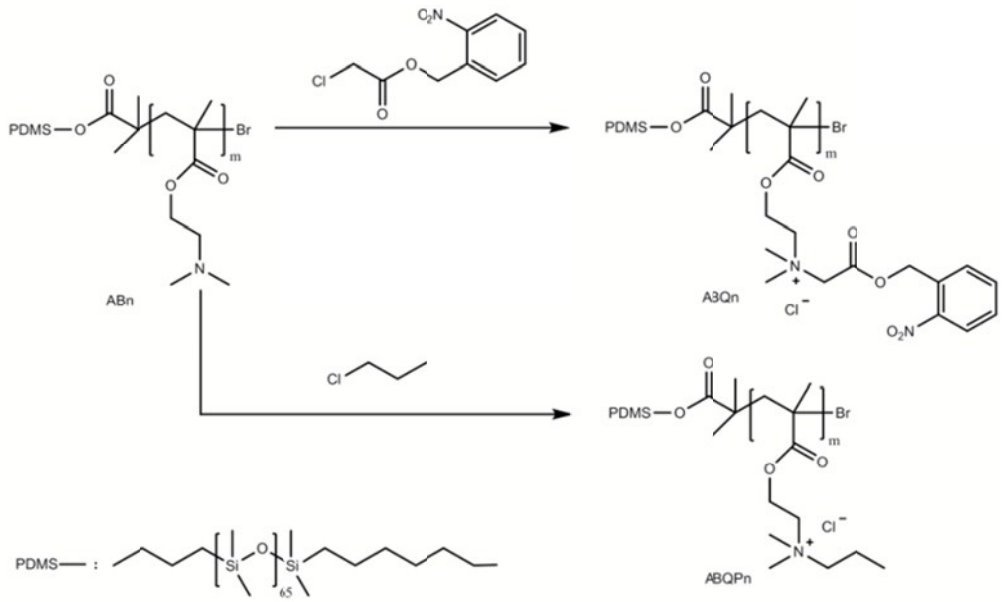


**Scheme 2.** Quaternization of ABn diblock copolymers with 2-nitrobenzyl-2-chloroacetate and 1-chloropropane, leading to positively charged ABQn (photo-cleavable) and ABQPn (non-cleavable) diblock copolymers.

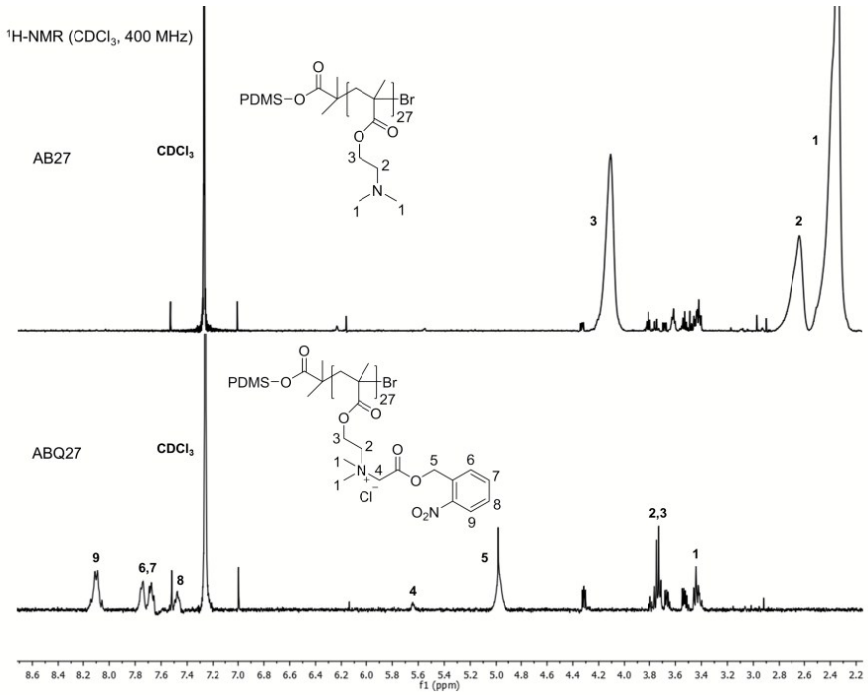


**Figure 1.** Partial $^{1}$H-NMR spectra of pristine (AB27) and photo-cleavable (ABQ27) diblock copolymers in the range 2.2 – 8.6 ppm, in $CDCl_3$, 400 MHz, containing the proton signals for the side-chain tertiary amine groups (top spectrum), and for the quaternary amine groups (bottom spectrum).

The $^{1}$H-NMR spectra of diblock copolymers quaternized with 1-chloropropane (ABQPn), showed insignificant changes compared with those of pristine PDMS-*b*-PDMAEMA, the presence of characteristic signals for the propyl protons being the only prove indicating the quaternization process occurred (Figure S3 and S4, peaks 5 and 6).

**Structural changes induced by UV irradiation**

As it was already presented in the literature in the case of homopolymers,[36,52,53] the 2-nitrobenzyl ester groups of the quaternized PDMAEMA block are expected to be cleaved under UV irradiation at a wavelength of 365 nm converting it from a cationic to a zwitterionic (carboxybetaine) block (Scheme 3).

In order to quantify the cleavage of 2-nitrobenzyl moieties, the photolytic degradation was followed by $^{1}$H-NMR spectroscopy on ABQ5, observing the spectral changes over an UV irradiation time of 60 minutes, at 365 nm (Figure 2). Unfortunately, no kinetics could be done for ABQ27, due to the poor solubility of longer charged block in $CDCl_3$ and high tendency to form aggregates even after the pre-filtration step. For the other copolymers, no structural changes were observed in $^{1}$H-NMR spectra after UV irradiation (not shown here).

The reaction proceeded rapidly in $CDCl_3$, the characteristic signals for the aromatic protons of the side-product, 2-nitroso benzaldehyde, appeared after 5 minutes of UV irradiation at $\delta$ = 6.44 (dd, 1H, peak a), 7.68 (dt, 1H, peak b), 7.91 (dt, 1H, peak c), 8.21 (dd, 1H, peak d), and 12.1 (s, 1H, CHO, peak e) ppm (Figure 2A), according to the literature.[62] Moreover, the signal at 4.99 ppm, corresponding to the protons of methylene group bound to the aromatic ring (-CO-O-C$\underline{H_2}$-$C_6H_4$-$NO_2$), disappeared after 30 minutes indicating that photolysis took place. In addition, the signal at 5.64 ppm, attributed to the protons of methylene group bound to the ammonium group (-$N^+(CH_3)_2$-C$\underline{H_2}$-CO-O-), was shifted to 5.57 ppm and its intensity increased over 30 minutes, remaining almost constant at later times, suggesting complete formation of the zwitterionic product (Figure 2A and 2B, peak f). However, the side-product, which is not soluble in $CDCl_3$, slowly separated from the solution and the corresponding peaks start to disappear after 10 min of UV irradiation.

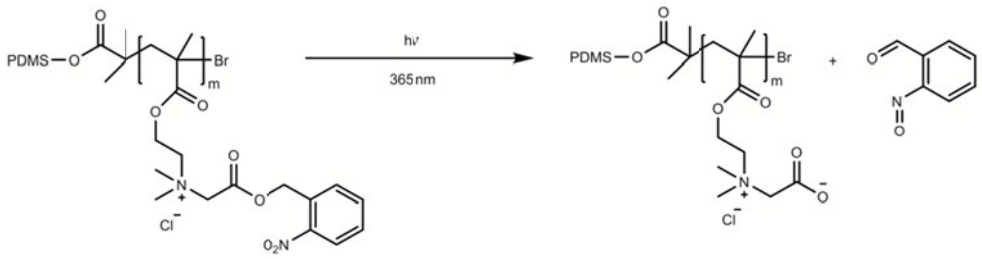


**Scheme 3.** Photo-cleavage of positively charged diblock copolymers, ABQn, by UV exposure, leading to neutral diblock copolymers.

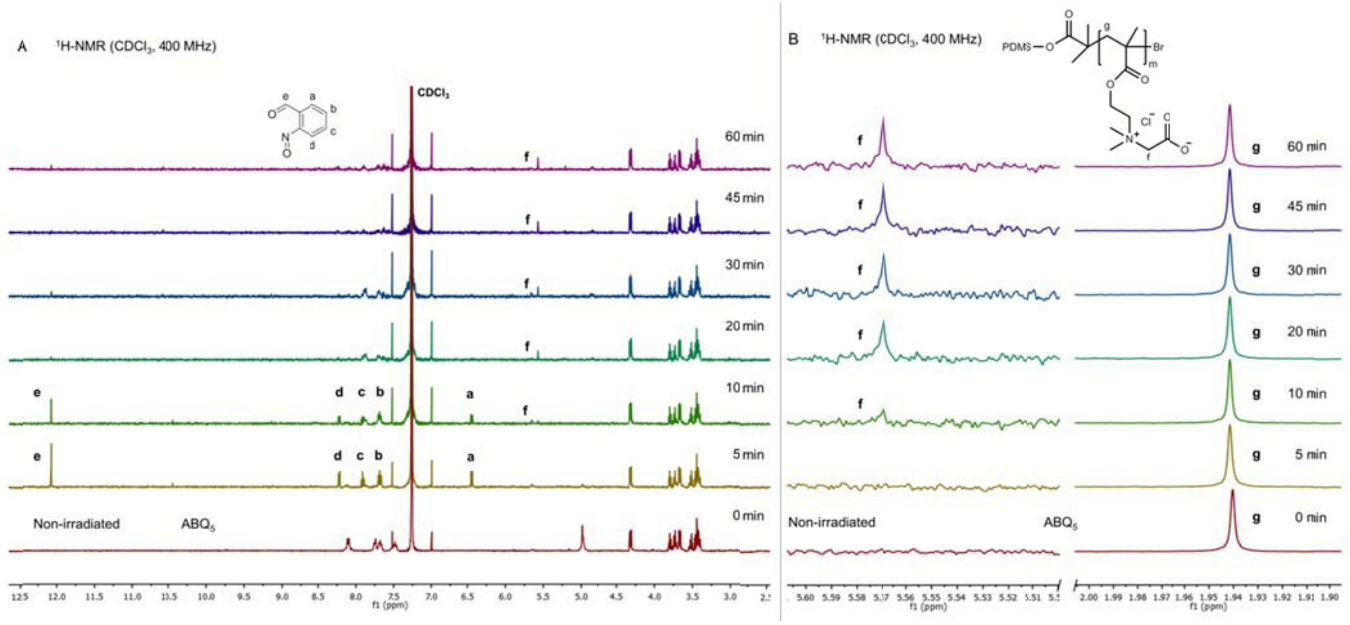


**Figure 2.** Partial $^{1}$H-NMR spectra of photo-cleavable ABQ5 diblock copolymer in $CDCl_3$, 400 MHz, showing the changes of proton signals corresponding to the pendant quaternary amine groups, over an irradiation time of 60 minutes: (A) Appearance of new proton peaks in the range 6.0-12.5 ppm (peaks a-e) corresponding to 2-nitroso benzaldehyde, the side-product formed during the UV exposure; (B) Variation of the proton peaks in the range 5.5-5.6 ppm (peak f), corresponding to the pendant methylene ($-N^{+}(CH_3)_2-C\underline{H}_2-CO-O^{-}$) group, compared to the peak at 1.94 ppm (peak g) assigned to the protons from the PDMAEMA backbone ($-C\underline{H}_2-C(CH_3)-CO-O-$).

To further evaluate the time for complete cleavage of the photo-labile groups, the peak integral of the methylene protons ($-N^{+}(CH_3)_2-C\underline{H}_2-CO-O^{-}$) at 5.57 ppm (peak f) was compared to the constant peak integral of the methylene protons from the PDMAEMA backbone ($-C\underline{H}_2-C(CH_3)-CO-O-$) at 1.94 ppm (peak g), taken as reference, because the polymer backbone remains unaffected by UV irradiation (Figure3).

A pseudo-first order rate constant, *k*, was calculated to be $(0.79 \pm 0.25) \times 10^{-3}$ $s^{-1}$ (half-time, $t_{1/2}$ = 883 s) by fitting the obtained data using a first exponential equation.[61] Accordingly, after 30 minutes of UV irradiation an almost constant value of about 100% was obtained for the degradation efficiency, indicating that complete photo-cleavage had occurred.

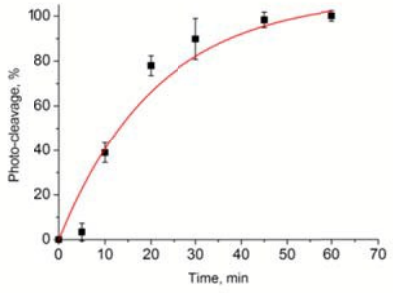


**Figure 3.** The time-dependent photolysis of ABQ5 monitored by integration of the new $^{1}$H-NMR signal at 5.57 ppm (peak f) corresponding to the ($-N^{+}(CH_3)_2-CH_2-CO-O^{-}$) protons, shifted during the UV exposure, taking as reference the constant integral of the protons from the PDMAEMA backbone ($-CH_2-C(CH_3)-CO-O-$, peak g). Error bars are shown as standard deviations of three individual measurements.

To optimize both the photo-cleavage yield and degradation time, the photolysis of ABQn copolymers was investigated in more polar media (ethanol and PBS), for times up to 60 min.

The difference between the photo-degradation process of solubilized polymer chains and those self-assembled into a nanostructure in aqueous solution was investigated by UV-Vis spectroscopy (Figure S6 A-D). The peak observed at 280 nm was decreasing during the photolysis reaction, indicating a decrease in the number of pendant 2-nitrobenzyl groups. This was accompanied by the formation of a 'shoulder' at 320 nm, corresponding to the side-product, 2-nitroso benzaldehyde, which gained intensity with the increase of the irradiation time.

To determine the extent of photo-cleavage, the relative absorbance of each solution or dispersion was monitored at 325 nm and plotted as a function of time (Figure 4). The photo-degradation kinetics data support the results obtained by $^{1}$H-NMR spectroscopy, suggesting a complete cleavage of the photo-labile groups in less than 30 minutes for both copolymers. The corresponding pseudo-first order rate constants, as well as the other photolysis parameters were calculated using the same equation,[61] and they showed that the photolysis process is dependent on the nature of the medium used to solve the copolymers or to induce their self-assembly, and the length of hydrophilic block (Table 1).

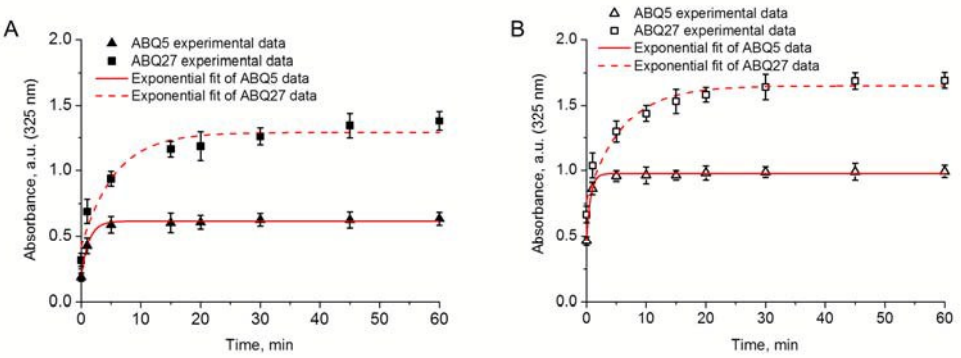


**Figure 4.** Photo-cleavage kinetics of ABQ5 (triangles) and ABQ27 (squares) copolymers in ethanol (A), and PBS (B), measuring the absorbance of solution or dispersion at 325 nm by UV-Vis spectroscopy after irradiation over time points between 0-60 min. Error bars are shown as standard deviations of triplicate (n = 3) measurements.

**Table 1.** The kinetic parameters obtained from fitting the photolysis data using a first order exponential equation.

| | Sample | $y_0$ | A | $k \times 10^3$ ($s^{-1}$) | $R^2$ | $t_{1/2}$ (s) |
|---|---|---|---|---|---|---|
| PBS | ABQ5 | 0.98 ± 0.01 | -0.51 ± 0.02 | 25.42 ± 2.30 | 0.99 | 27 |
| | ABQ27 | 1.65 ± 0.04 | -0.88 ± 0.07 | 2.77 ± 0.64 | 0.95 | 250 |
| EtOH | ABQ5 | 0.62 ± 0.01 | -0.43 ± 0.02 | 13.08 ± 1.46 | 0.99 | 53 |
| | ABQ27 | 1.29 ± 0.05 | -0.87 ± 0.09 | 2.99 ± 1.02 | 0.93 | 232 |

Thus, when copolymers are dissolved in EtOH or dispersed in PBS (pH 7.4), the complete photo-cleavage occurred much faster, in less than 10 minutes, compared to the photo-degradation in $CDCl_3$, followed by $^1$H-NMR spectroscopy. This difference is due to the polarity of these protic solvents, which is expected to determine a higher photo-degradation rate of pendant 2-nitrobenzyl groups into 2-nitroso benzaldehyde side-product.[63] However, the influence of the solvent nature on the photo-degradation rate is clearly seen in the case of the shorter ABQ5 copolymer, which has a degradation rate constant in PBS two times higher than in ethanol, that means water molecules induce a faster cleavage of the nitrobenzyl ester groups.

Even though the presence of aqueous environment is known to facilitate the photo-cleavage leading to an increase of photo-degradation rate,[64] the longer hydrophilic block of ABQ27 and the presence of more π-π and cation-π interactions between the pendant groups, favoured by the self-assembly process, caused a slight decrease of degradation rate constant for this copolymer in PBS compared to that in ethanol.

**Effect of quaternization and UV irradiation on nanoparticle morphology, size, and zeta potential**

DLS and TEM were used to study the change in morphology of self-assembled nanoparticles in PBS, before and after UV irradiation (Table 2). Unfortunately, a more detailed investigation by static light scattering (SLS) was not possible due to the nanoparticle degradation under long exposure to the laser light of the equipment.

The average diameter of the self-assembled nanoparticles was affected after quaternization, depending on the nature of substituent bound to the pendant moieties (Table 2, Figures 5 and S7). The obvious decrease in size observed in the case of photo-labile self-assembled nanoparticles (ABQn) could be attributed to the stronger π-π and cation-π interactions of aromatic nitrobenzyl rings compared to the hydrophobic interaction between propyl groups (ABQPn). The decrease is more evident for the photo-labile copolymer assemblies with a longer quaternized PDMAEMA block (ABQ27), where the higher number of pendant aromatic groups overwhelmed the electrostatic repulsion between the cationic charges. This induced the formation of smaller, more compact nanoparticles (Figures 5 and S7), which may also slow down the photo-cleavage process, due to the sterically hindered access of water molecules to the photo-degradable groups.

**Table 2.** The size and zeta potential values of 3D polymeric assemblies before and after UV irradiation, in PBS [1 mg $mL^{-1}$].

| Sample | before UV irradiation | | | | after UV irradiation | | | |
|---|---|---|---|---|---|---|---|---|
| | Size[a] [nm] | Size[b] [nm] | PDI | ζ [mV] | Size[a] [nm] | Size[b] [nm] | PDI | ζ [mV] |
| AB5 | 201 ± 4 | 75 ± 19 | 0.198 | 23 ± 2 | 223 ± 7 | 91 ± 14 | 0.278 | 20 ± 2 |
| ABQ5 | 132 ± 1 | 70 ± 5 | 0.166 | 11 ± 1 | 136 ± 3 | 75 ± 4 | 0.217 | 0 ± 0.6 |
| ABQP5 | 185 ± 4 | 128 ± 3 | 0.244 | 21 ± 1 | 198 ± 6 | 139 ± 9 | 0.325 | 21 ± 1 |
| AB27 | 116 ± 2 | 84 ± 4 | 0.271 | 19 ± 1 | 119 ± 2 | 85 ± 7 | 0.217 | 17 ± 1 |
| ABQ27 | 87 ± 1 | 35 ± 2 | 0.196 | 13 ± 1 | 94 ± 2 | 40 ± 2 | 0.222 | 3 ± 1 |
| ABQP27 | 184 ± 4 | 117 ± 11 | 0.146 | 16 ± 1 | 185 ± 6 | 120 ± 10 | 0.167 | 16 ± 1 |

[a] Determined using DLS as intensity-averaged size; [b] Determined using DLS as number-averaged size.

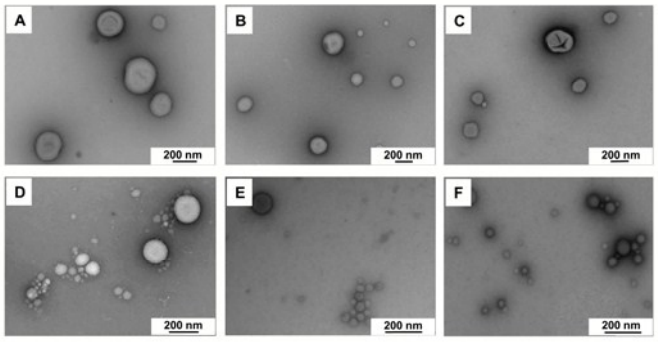


**Figure 5.** TEM micrographs of nanoparticles based on AB5 (A), ABQ5 before (B) and after irradiation (C), AB27 (D), ABQ27 before (E) and after irradiation (F).

In the case of propyl-modified block copolymer, ABQP5, the decrease in size is less significant, while for ABQP27, the increased number of propyl pendant groups does not induces a further decrease in size, which means that the hydrophobic interactions of propyl substituents are not strong enough to shield the electrostatic repulsion between the positively charged groups (Table 2, Figure S7).

Upon UV irradiation, the presence of self-assembled structures proves that the nanoparticles are not destroyed and stable after 30 minutes of UV irradiation with a light intensity of 10 mW $cm^{-2}$ (Figure 5 C and F, as well as Figure S7 C' and F'). However, the average size of nanoparticles with longer non-cleavable hydrophilic blocks increased in average by 3-7 nm, while this increase was much higher (around 15-20 nm) for nanoparticles with a shorter hydrophilic block (Table 2). The increase in size and polydispersity might be induced by the increase in temperature from 25°C up to 32°C during UV exposure, favouring the hydrophobic interactions and inducing rearrangements of polymers chains. In the case of photo-labile self-assemblies, a minor second population of large aggregates (maximum 3% of intensity) with a size of 1000-1300 nm was observed by DLS, formed by the side product, 2-nitroso benzaldehyde, after UV exposure.

A comparison of ζ potential data showed a similar pattern; a decrease after quaternization and self-assembly in PBS solution, the tendency being more prevalent for photo-labile copolymer nanoparticles (Table 2). This again shows that the benzyl substituents have the potential to form stronger attractive interactions, within the self-assembled structures, with each other (π-π stacking),[65] as well as with the quaternary groups (cation–π),[66] than the hydrophobic interactions of propyl moieties, for copolymers with similar hydrophilic block length, leading to lower ζ potential values.

The photo-cleavage was also confirmed by ζ potential measurements, which showed a decrease of the potential down to almost neutral after irradiation, thereby confirming the formation of zwitterionic carboxybetaine groups. The conversion into the zwitterionic form and the cleavage of the aromatic side-chain would be expected to disrupt the nanoparticle architecture. However, the presence of the hydrophobic block, PDMS, does not allow the self-assembled structures to fall apart.

No significant change of ζ potential was observed for the pristine and propyl-quaternized nanoparticles after UV exposure, because they do not have cleavable groups (Table 2).

**Cytotoxicity of pristine and modified polymers**

Formation of zwitterionic species after the UV irradiation of cationic photo-labile copolymers was expected to reduce the interaction of self-assembled structures with the cell membrane leading to decreased cytotoxicity.[52,53]

Cell viability was compared between ABn, ABQn, and ABQPn by the MTS cell viability assay. HeLa cells were cultured in the presence of nanoparticles at concentrations ranging from 50 to 300 μg $mL^{-1}$. Insignificant cell toxicity was observed for both quaternized and non-quaternized nanoparticles assembled with short copolymers AB5, ABQ5, and ABQP5 (Figure 6, left panel), in agreement with previous results on small cationic AB block polymers.[23]

The increased number of positive charges per copolymer chain by lengthening the hydrophilic block led to concentration dependent toxicity with complete cell death observed for polymer concentrations above 100 μg $mL^{-1}$ (approx. 6% cell viability).

However, unlike the other polycationic diblock copolymers, we show in our study that the modification of tertiary amine groups to quaternized photo-responsive moieties reduced cytotoxicity across all concentrations up to 300 μg $mL^{-1}$ (about 90% cell viability) (Figure 6, right panel). Moreover, ABQn nanoparticles showed limited toxicity also after UV-irradiation, suggesting the final cleavage side-product (2-nitroso benzaldehyde) does not lead to toxicity (Figure S9). This improvement in cell viability of photo-responsive copolymers could be attributed to the substantial decrease in number of charges able to interact with the cell membrane, due to the steric hindrance determined by π-π stacking and cation–π interaction of pendant 2-nitrobenzyl quaternary groups within the self-assembled nanoparticles. The decrease of available charges is known to lower toxicity (seen often by masking positive charges with PEG),[28,29] but it could also be argued the decrease in surface charge led to lower cell surface interaction with the negative cell surface glycosaminoglycans leading to decreased uptake and lower toxicity.

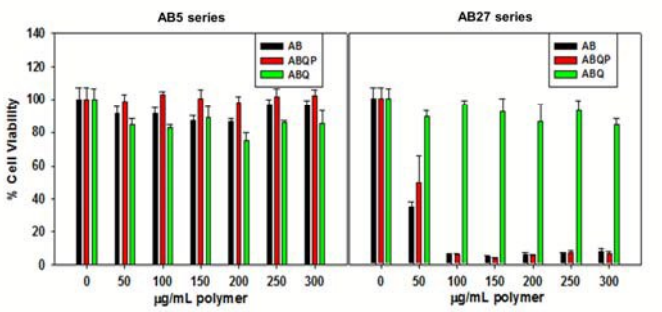


**Figure 6.** HeLa cell growths versus concentration of polymer solutions after 24 h. Error bars are shown as standard deviations of three individual (n = 3) measurements.

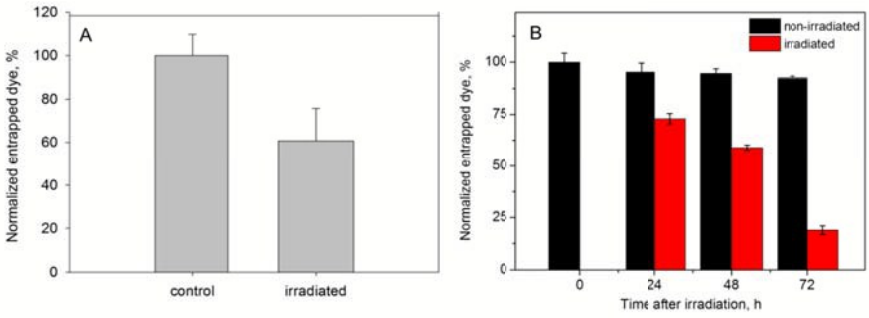


Figure 7. The amount of entrapped dye (%) in the ABQ27 nanoparticles after 30 minutes of UV irradiation compared to the non-irradiated samples and determined after 24 h of release by UV-Vis spectroscopy (A) or at various time points of release by fluorimetry (B).

To test this possibility, the quaternized ABQP27 copolymer was also investigated. The propyl-modified particles showed similar toxicity to the AB27-based nanoparticles (Figure 6). This suggests that the decrease in toxicity is caused by the nature of interactions between the cationic pendant groups, which plays an important role even before being cleaved into the zwitterionic form. Lowering the cell toxicity of ABQn block copolymers, even when the length of positively charged block is extended, makes these polymeric nanoparticles an improved and promising delivery system compared to current polycationic vectors.

**SRB entrapment and in vitro release**

The interaction of cationic block copolymers with oppositely charged molecules was studied with sulforhodamine B (SRB), as model anionic compound. SRB is an anionic dye with two sulfonic groups and is known to electrostatically bind on protein basic amino acid residues.[67] Its incorporation into a nanocarrier system is dominated by electrostatic interactions rather than hydrophobic ones.

Interaction of SRB with cationic photo-cleavable copolymers during the self-assembly process was followed by UV-Vis spectroscopy. SRB entrapment efficiency was extremely low and below the detection limit for AB5 and ABQ5 copolymers (data not shown). Because both copolymers have a short PDMAEMA block in their structure (5 repeating units), the number of positive charges was not high enough to efficiently bind SRB. The SRB entrapment during the self-assembly of copolymer chains with AB27 and ABQ27 was much more efficient due to the longer cationic block. However, the dye loading efficiency (DLE) of ABQ27 was much higher (approx. 20%, w/w) in comparison to AB27 (< 5%, w/w) indicating that not only the length of the charged hydrophilic block is important, but also the nature of cationic groups in the ABQ system. The cationic block containing quaternary ammonium groups is considered to be a stronger polyelectrolyte compared to the other cationic block with the same length containing tertiary ammonium groups. Therefore, the interaction of the quaternized ABQ27 with the sulphate groups of SRB was stronger, and a higher DLE was observed.

*In vitro* dye release from SRB-loaded ABQ27 nanoparticles was investigated in PBS buffer after purification by dialysis to remove the free dye. The residual dye content was evaluated by UV-Vis measurements at 565 nm, taking into account the extinction coefficient corresponding to ABQ27-SRB complex.

As can be observed from the normalized values of remaining dye in the nanoparticles, approximately 40% (w/w) of dye is released from ABQ27 after UV exposure and 24 h of dialysis, compared with the non-irradiated nanoparticles (Figure 7A). To have a better understanding on the release kinetics of SRB, the residual dye content was evaluated by fluorescence spectroscopy after 24 h, 48 h, and 72 h (Figure 7B).

The change in fluorescence intensity of entrapped dye was evaluated for both irradiated and non-irradiated nanoparticles. This was done to further provide evidence on the dye release caused solely by the charge shift of the irradiated nanoparticles compared to uncontrolled release due to the salts present in the PBS buffer which could affect the electrostatic interactions between the charged ABQ27 nanoparticles and the negatively charged dye.

Non-irradiated SRB-loaded nanoparticles showed a decrease of the dye content after 48 h of dialysis of about 5%, due to non-stimuli mediated release of SRB, with another 3% loss of dye after 48 and 72 h (Figure 7B). Importantly, the fluorescence intensity of the irradiated SRB-loaded ABQ27 nanoparticles decreased significantly after 24 and 48 h reaching a maximal dye release efficiency (DRE) after 72 h (about 30%, 40%, and 80% dye release respectively). The conversion into the zwitterionic form would be expected to quickly stop the interaction of anionic dye with the polymer and to cause a rapid release. Nevertheless, it was already shown by DLS and TEM imaging that while irradiation changes the overall charge, it does not disrupt the particle architecture. Therefore, the photo-cleavage cannot rapidly break the spatial barrier of the pre-formed nanoparticles and cause a rapid release, but instead causes the dye to slowly diffuse out over time. In conclusion, this system has overcome some of the major barriers previously seen with other cationic nanocarriers, like cytotoxicity and burst release after the application of the triggering stimulus.

**Cell uptake of SRB-loaded ABQ27 nanoparticles**

To analyse how converting the cationic pendant groups into zwitterionic moieties would affect delivery characteristics, cell uptake assays were performed.

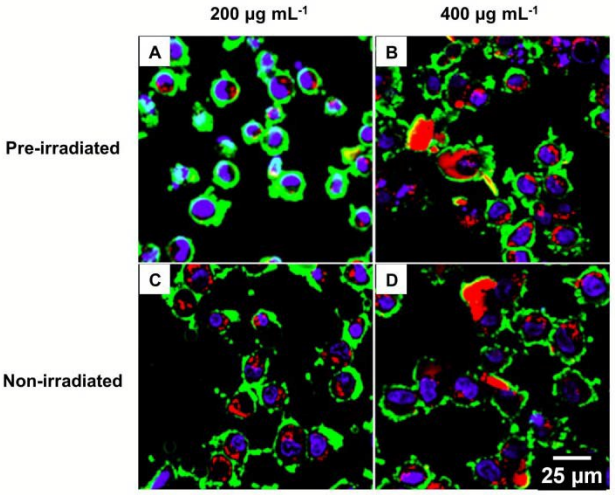


**Figure 8.** SRB-loaded ABQ27 nanoparticles, 200 or 400 µg mL$^{-1}$, incubated on HeLa cells for 24 h, after 30 minutes of pre-irradiation (A and B respectively) or without pre-irradiation (C and D respectively). All CLSM micrographs have the same magnification.

Cells were incubated with SRB-loaded ABQ27 nanoparticles (200 µg mL$^{-1}$) that were irradiated for 30 minutes (to create the zwitterionic species) or with non-irradiated nanoparticles (Figure 8A and 8C respectively).

The ABQ27 nanoparticles irradiated before adding them to the cells showed a slight uptake into cells over 24 hours (Figure 8A). In contrast, the cells treated with non-irradiated nanoparticles showed a significantly more signal for the SRB across a larger portion of the cells (Figure 8C and S10). This trend could be caused by two effects. First, the change in charge leads to release of the dye, so that even though the nanoparticles are uptaken they are not seen; however, the release data suggests that in the time it takes for most uptake to begin (~ 4 hours) the dye should not have been released prior to entering the cells. Therefore, the second, most probable, effect is that the transformation of the positively charged surface of the nanoparticles into a neutral surface by cleavage of the light sensitive groups leads to less interaction with the cell surface and lower uptake as is expected for non-cationic nanoparticles. It is apparent that the cell shape is slightly irregular compared to untreated controls (Figure S10).

By increasing the dose to 400 µg mL$^{-1}$, a greater uptake is seen in both samples; however, it is apparent the cells begin to become apoptotic. To validate this, further cell viability assays were performed for the higher doses showing that indeed a dosage of 400 µg mL$^{-1}$ is becoming toxic (50% cell viability), but that the irradiated samples are less so (70% cell viability) (Figure S11).

## Conclusions

We have synthesized novel amphiphilic diblock copolymers containing photo-cleavable nitrobenzyl moieties by a combination of ATRP and post-polymerization modification, which can undergo a structural transformation from cationic to zwitterionic, triggered by UV light. Nanoparticles with entrapped SRB were obtained by self-assembly in aqueous solutions, and were able to release it in a photo-responsive manner. The conversion of the nanoparticles into the zwitterionic form would be expected to quickly release the model dye. However, the irradiation changes the overall charge, but it does not disrupt the particle architecture, causing a slow dye release, process controlled only by the diffusion of drug out of self-assembled nanocarriers. ABQn-based nanoparticles were non-toxic for cells both before and after UV irradiation up to a dose of 300 µg mL$^{-1}$ compared to propyl-quaternized nanostructures, suggesting that the decrease in toxicity is caused by the nature of the quaternization agent that also plays an important role in the self-assembly of the nanoparticles and the release mechanism of the loaded dye. Quaternized PDMS-*b*-PDMAEMA polymeric nanoparticles have overcome the major barriers (*e.g.* toxicity, binding, stimuli-triggered release) previously seen with other cationic nanocarriers to deliver negatively charged payloads in a photo-mediated manner. This is the first study that successfully designed cationic delivery systems which irreversibly change to a neutral form, slowly releasing cargo after exposure to light as a triggered stimulus while remaining non-toxic. These results indicate the high potential of these cationic polymeric systems as photo-responsive nanocarriers for sustained, controlled drug delivery.

## Acknowledgements

The Swiss National Science Foundation (150059), the National Centre of Competence in Research "Molecular Systems Engineering" (51NF4O_141825), the Marie Curie Action – Intra-European Fellowship (p.n. 301398) and University of Basel are acknowledged for financial support. The authors thank Gabriele Persy for TEM measurements, and A.D. gratefully acknowledges Dr. Gesine Gunkel-Grabole and Samuel Lörcher from University of Basel for useful discussions. We also thank Mihai Lomora for designing the graphical abstract and artistic illustration of the concept.

## Notes and references

1 Y. Mai and A. Eisenberg, *Chem. Soc. Rev.*, 2012, **41**, 5969.
2 J. Kowal, X. Zhang, I. A. Dinu, C. G. Palivan and W. Meier, *ACS Macro Lett.*, 2013, **3**, 59.
3 K. Kataoka, A. Harada and Y. Nagasaki, *Adv. Drug Del. Rev.*, 2001, **47**, 113.
4 G. Gunkel-Grabole, S. Sigg, M. Lomora, S. Lorcher, C. G. Palivan and W. P. Meier, *Biomater. Sci.*, 2015, **3**, 25.
5 A. Rösler, G. W. M. Vandermeulen and H.-A. Klok, *Adv. Drug Del. Rev.*, 2012, **64 Suppl.**, 270.
6 H. Cabral and K. Kataoka, *J. Control. Release*, 2014, **190**, 465.
7 J. S. Lee and J. Feijen, *J. Control. Release*, 2012, **161**, 473.
8 Z. Ge and S. Liu, *Chem. Soc. Rev.*, 2013, **42**, 7289.
9 R. Srikar, A. Upendran and R. Kannan, *WIREs Nanomed. Nanobiotechnol.*, 2014, **6**, 245.
10 T. Ren, Q. Liu, H. Lu, H. Liu, X. Zhang and J. Du, *J. Mater. Chem.*, 2012, **22**, 12329.
11 L. Che, J. Zhou, S. Li, H. He, Y. Zhu, X. Zhou, Y. Jia, Y. Liu, J. Zhang and X. Li, *Int. J. Pharm.*, 2012, **439**, 307.

12 F. Bucatariu, C.-A. Ghiorghita and E. S. Dragan, *Colloids Surf. B. Biointerfaces*, 2015, **126**, 224.
13 X. Guo and L. Huang, *Acc. Chem. Res.*, 2011, **45**, 971.
14 L. Jin, X. Zeng, M. Liu, Y. Deng and N. He, *Theranostics*, 2014, **4**, 240.
15 N. Alizadeh and E. Shamaeli, *Electrochim. Acta*, 2014, **130**, 488.
16 S. K. Samal, M. Dash, S. van Vlierberghe, D. L. Kaplan, E. Chiellini, C. van Blitterswijk, L. Moroni and P. Dubruel, *Chem. Soc. Rev.*, 2012, **41**, 7147.
17 Q. Zeng, H. Jiang, T. Wang, Z. Zhang, T. Gong and X. Sun, *J. Control. Release*, 2015, **200**, 1.
18 Y. Kodama, Y. Shiokawa, T. Nakamura, T. Kurosaki, K. Aki, H. Nakagawa, T. Muro, T. Kitahara, N. Higuchi and H. Sasaki, *Biol. Pharm. Bull.*, 2014, **37**, 1274.
19 O. Samsonova, C. Pfeiffer, M. Hellmund, O. M. Merkel and T. Kissel, *Polymers*, 2011, **3**, 693.
20 J. Cai, Y. Yue, D. Rui, Y. Zhang, S. Liu and C. Wu, *Macromolecules*, 2011, **44**, 2050.
21 E. Bilensoy, *Expert Opin. Drug Deliv.*, 2010, **7**, 795.
22 C. H. Jones, C.-K. Chen, A. Ravikrishnan, S. Rane and B. A. Pfeifer, *Mol. Pharm.*, 2013, **10**, 4082.
23 A. Car, P. Baumann, J. T. Duskey, M. Chami, N. Bruns and W. Meier, *Biomacromolecules*, 2014, **15**, 3235.
24 Y. Zhang, A. Aigner and S. Agarwal, *Macromol. Biosci.*, 2013, **13**, 1267.
25 J. Hu, G. Zhang, Z. Ge and S. Liu, *Prog. Polym. Sci.*, 2014, **39**, 1096.
26 X. J. Loh, S. J. Ong, Y. T. Tung and H. T. Choo, *Macromol. Biosci.*, 2013, **13**, 1092.
27 M. Cai, M. Leng, A. Lu, L. He, X. Xie, L. Huang, Y. Ma, J. Cao, Y. Chen and X. Luo, *Colloids Surf. B. Biointerfaces*, 2015, **126**, 1.
28 S. Lin, F. Du, Y. Wang, S. Ji, D. Liang, L. Yu and Z. Li, *Biomacromolecules*, 2007, **9**, 109.
29 Y. Qiao, Y. Huang, C. Qiu, X. Yue, L. Deng, Y. Wan, J. Xing, C. Zhang, S. Yuan, A. Dong and J. Xu, *Biomaterials*, 2010, **31**, 115.
30 M. Barz, R. Luxenhofer, R. Zentel and M. J. Vicent, *Polym. Chem.*, 2011, **2**, 1900.
31 V. Kumar and D. Kalonia, *AAPS PharmSciTech*, 2006, **7**, E47.
32 H.-J. Sung, P. Chandra, M. D. Treiser, E. Liu, C. P. Iovine, P. V. Moghe and J. Kohn, *J. Cell. Physiol.*, 2009, **218**, 549.
33 T. Ishida and H. Kiwada, *Int. J. Pharm.*, 2008, **354**, 56.
34 Z. Cao and S. Jiang, *Nano Today*, 2012, **7**, 404.
35 Q. Jin, Y. Chen, Y. Wang and J. Ji, *Colloids Surf. B. Biointerfaces*, 2014, **124**, 80.
36 Q. Jin, T. Cai, Y. Wang, H. Wang and J. Ji, *ACS Macro Lett.*, 2014, **3**, 679.
37 F. Abbasi, H. Mirzadeh and A.-A. Katbab, *Polym. Int.*, 2001, **50**, 1279.
38 E. Yilgör and I. Yilgör, *Progr. Polym. Sci.*, 2014, **39**, 1165.
39 F. Itel, M. Chami, A. Najer, S. Lörcher, D. Wu, I. A. Dinu and W. Meier, *Macromolecules*, 2014, **47**, 7588.
40 A. Najer, D. Wu, D. Vasquez, C. G. Palivan and W. Meier, *Nanomedicine*, 2013, **8**, 425.
41 J. Zhang, X. Li and X. Li, *Prog. Polym. Sci.*, 2012, **37**, 1130.
42 S. Deshayes and A. M. Kasko, *J. Polym. Sci., Part A: Polym. Chem.*, 2013, **51**, 3531.
43 A. Feng and J. Yuan, *Macromol. Rapid Commun.*, 2014, **35**, 767.
44 W. Cheng, L. Gu, W. Ren and Y. Liu, *Mater. Sci. Eng. C*, 2014, **45**, 600.
45 E. Cabane, X. Zhang, K. Langowska, C. Palivan and W. Meier, *Biointerphases*, 2012, **7**, 1.
46 M. D. Green, A. A. Foster, C. T. Greco, R. Roy, R. M. Lehr, I. I. I. T. H. Epps and M. O. Sullivan, *Polym. Chem.*, 2014, **5**, 5535.
47 J.-F. Gohy and Y. Zhao, *Chem. Soc. Rev.*, 2013, **42**, 7117.
48 J.-M. Schumers, C.-A. Fustin and J.-F. Gohy, *Macromol. Rapid Commun.*, 2010, 31, 1588.
49 E. Cabane, V. Malinova, S. Menon, C. G. Palivan and W. Meier, *Soft Matter*, 2011, **7**, 9167.
50 B. Yan, J.-C. Boyer, N. R. Branda and Y. Zhao, *J. Am. Chem. Soc.*, 2011, **133**, 19714.
51 X. Wang, G. Liu, J. Hu, G. Zhang, and S. Liu, *Angew. Chem. Int. Ed.*, 2014, **53**, 3138.
52 P. Sobolčiak, M. Špírek, J. Katrlík, P. Gemeiner, I. Lacík and P. Kasák, *Macromol. Rapid Commun.*, 2013, **34**, 635.
53 A. Sinclair, T. Bai, L. R. Carr, J.-R. Ella-Menye, L. Zhang and S. Jiang, *Biomacromolecules*, 2013, **14**, 1587.
54 X. Wang, J. Hu, G. Liu, J. Tian, H. Wang, M. Gong, and S. Liu, *J. Am. Chem. Soc.*, 2015, **137**, 15262.
55 J. Dong, Y. Wang, J. Zhang, X. Zhan, S. Zhu, H. Yang and G. Wang, *Soft Matter*, 2013, **9**, 370.
56 J. Dong, R. Zhang, H. Wu, X. Zhan, H. Yang, S. Zhu and G. Wang, *Macromol. Rapid Commun.*, 2014, **35**, 1255.
57 J. V. Natarajan, C. Nugraha, X. W. Ng and S. Venkatraman, *J. Control. Release*, 2014, **193**, 122.
58 D. M. Haddleton, M. C. Crossman, B. H. Dana, D. J. Duncalf, A. M. Heming, D. Kukulj and A. J. Shooter, *Macromolecules*, 1999, **32**, 2110.
59 P. J. Serafinowski and P. B. Garland, *J. Am. Chem. Soc.*, 2003, **125**, 962.
60 D. Y. Wong, T. Ranganath and A. M. Kasko, *PLoS ONE*, **10**, e0139307.
61 A. M. Piggott and P. Karuso, *Tetrahedron Lett.* 2005, **46**, 8241.
62 Y. V. Il'ichev, M. A. Schwörer and J. Wirz, *J. Am. Chem. Soc.*, 2004, **126**, 4581.
63 M. S. Kim and S. L. Diamond, *Bioorg. Med. Chem. Lett.*, 2006, **16**, 4007.
64 A. P. Pelliccioli and J. Wirz, *Photochem. Photobiol. Sci.*, 2002, **1**, 441.
65 C. R. Martinez and B. L. Iverson, *Chem. Sci.*, 2012, **3**, 2191.
66 A. S. Mahadevi and G. N. Sastry, *Chem. Rev.*, 2013, **113**, 2100.
67 W. Voigt, Sulforhodamine B Assay and Chemosensitivity. In *Chemosensitivity*; Blumenthal, R. D., Ed. Methods in Molecular Medicine 110; Humana Press: Totowa, New Jersey, 2005; p 39.

Graphical Abstract

# Engineered non-toxic cationic nanocarriers with photo-triggered slow-release properties

*Ionel A. Dinu,* Jason T. Duskey, Anja Car, Cornelia G. Palivan, Wolfgang Meier**

A simple and versatile strategy using cationic amphiphilic diblock copolymers synthesized by a combination of ATRP and post-polymerization quaternization to prepare photo-responsive nanocarriers showing slow-release properties and low cytotoxicity was reported.